A Gold Rush: Designing Hydrogels for Selective Recovery in Wastewater Containing Mixed Metal Ions

ACS APPLIED MATERIALS & INTERFACES

www.acsami.org
Research Article

A Gold Rush: Designing Hydrogels for Selective Recovery in Wastewater Containing Mixed Metal Ions

Pamela Cinfrignini, Alice Boschetti,* Giacomo Ghini, Alice Tenti, Marie Plazanet, Daniele Martella,* and Renato Torre

Cite This: *ACS Appl. Mater. Interfaces* 2024, 16, 68368−68378
Read Online

ABSTRACT: The use of synthetic hydrogels in wastewater treatment represents a promising and scalable approach to achieving clean water. By modulation of their chemical structure, hydrogels can effectively remove a wide range of toxic compounds, including emerging organic pollutants and heavy metals. For the latter, recovery is essential for both environmental protection and metal recycling. The increasing demand for gold, a nonrenewable metal widely used in many technologies, calls for methods for its selective recovery from complex metal cation solutions. This study explores easy-to-make poly(acrylamide-*co*-acrylic acid) hydrogels as adsorbents for gold recovery from industrial wastewater containing other precious metals. Such material can reduce gold cations into elemental nanoparticles and microparticles in acid environments at room temperature. This process offers a potential route for metal recovery that is not based on weak interaction or complex formation. Batch tests demonstrate a good adsorption capacity (up to 124 mg/g) and efficient separation from other precious metal ions (Ru, Ir, Pd, Pt, and Rh) in a solution that closely mimics realistic industrial waste conditions. These hydrogels would enable gold recovery also from other complex metal solutions, including those derived from the dissolution of electronic wastes.

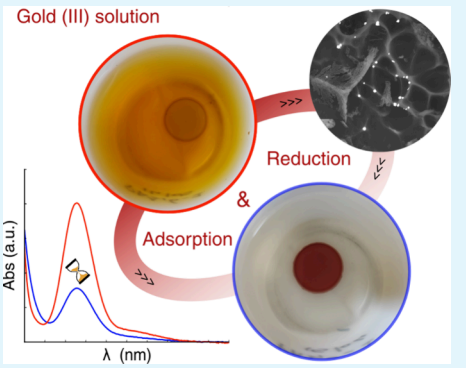

KEYWORDS: *hydrogels, gold recovery, polyacrylamide, acrylic acid, gold nanoparticles, water treatments*

1. INTRODUCTION

Due to its outstanding physical and chemical attributes such as ductility, conductivity, and catalytic properties, gold is heavily employed in many fields, including industrial manufacturing, electronics, and medicine.[1] In 2023, the demand for gold exceeded its previous record, reaching 4.89 kilotons, excluding OTC (over-the-counter), with the jewelry industry accounting for nearly 49% of global gold demand.[2,3] The increasing demand for gold is also accompanied by the urgent need of simple methods for its recovery and recycling, due to the nonrenewable nature of the material. Of particular interest is the selective recovery of gold from waste sources including electronic waste and industrial wastewater. In the waste solution, a given metal is often present in a mixture with other metals. For industrial processes such as gold plating and extraction, the concentration of gold in waste liquids is typically low, sometimes down to trace amounts. Moreover, these waste waters contain various metal ions or salts, which further complicates the recovery of gold.[4] Currently, recovery methods widely employed by industries for metal mixtures involve leaching solutions with multiple cycles of dissolution and activated carbons or ion exchange resins.[5] This last kind of resin has seen an increased employment due to their good versatility, improved gold recoveries from preg-robbing ores, better selectivity over base metals, and moreover, simple and energy-efficient elution/regeneration.[6,7] Indeed, resins are stripped at relatively low temperatures of around 60 °C, while activated carbon is eluted at 120−130 °C.[8] However, gold recovery following the elution process, as well as selectivity, still needs substantial enhancements. Other drawbacks include the high costs of materials and the energy expenses for combustion.

At the moment, adsorption is considered one of the most promising methods for its low cost, easy operation, as well as environmentally friendly characteristics.[9] The mechanism of adsorption broadly includes chemisorption, complexation, adsorption on surface, diffusion through pores, and ion exchange. In the past decade, numerous nanosized adsorbents (including core−shell nanoparticles or nanoflakes)[10] have been prepared exhibiting good performances in terms of adsorption capacity and selectivity. However, the nanosized dimension makes the recovery of the adsorbents itself extremely tricky,

Received: September 12, 2024
Revised: October 28, 2024
Accepted: October 29, 2024
Published: November 25, 2024

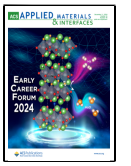

Table 1. Example of Poly(acrylamide-co-acrylic acid) Hydrogel for Water Treatment

Adsorbed species	Other Additives[a]	Main features	ref
Methylene Blue	Calcium hydroxide nanoparticles	Q_e[b] = 1056 mg/g (at pH = 7)	22
Methyl Violet	Attapulgite	Q_e = 1194 mg/g; Constant performance in the whole pH range 4.5 to 9.8	23
Methylene Blue, Methyl Orange, Pb^{2+}	–	Q_e and adsorption rate increase more than 10 times with high entangled network	24
Cu^{2+}	–	Q_e = 121 mg/g (at pH = 3)	25
Fe^{3+}, Cr^{3+}, Hg^{2+}	–	Test on single metal solution; Fe^{3+}: Q_e = 276 mg/g; Cr^{3+}: Q_e = 139 mg/g; Optimal pH > 5	26
Pb^{2+}, Cd^{2+}	Zeolites	Recovery of up to 99% for both metal (for pH above 5 in single ion solution)	27
Pb^{2+}, Cu^{2+}, Cd^{2+}	Microcrystalline cellulose	pH = 5 more suitable for metal recovery (test on single ion solution); Cu^{2+}: Q_e = 177 mg/g; Pb^{2+}: Q_e = 557 mg/g; Cd^{2+}: Q_e = 306 mg/g	28
Au^{3+}	–	Q_e = 124 mg/g (pH = 1). Competition test with other metals (Pt^{4+}, Rh^{3+}, Ir^{3+}, Pd^{2+}, Ru^{3+})	This work

[a]Compounds contained beyond poly(acrylamide-co-acrylic acid). [b]Q_e is the adsorption capacity at equilibrium calculated considering the equilibrium gold concentration C_e as $C_{t=250h}$ in eq 1.

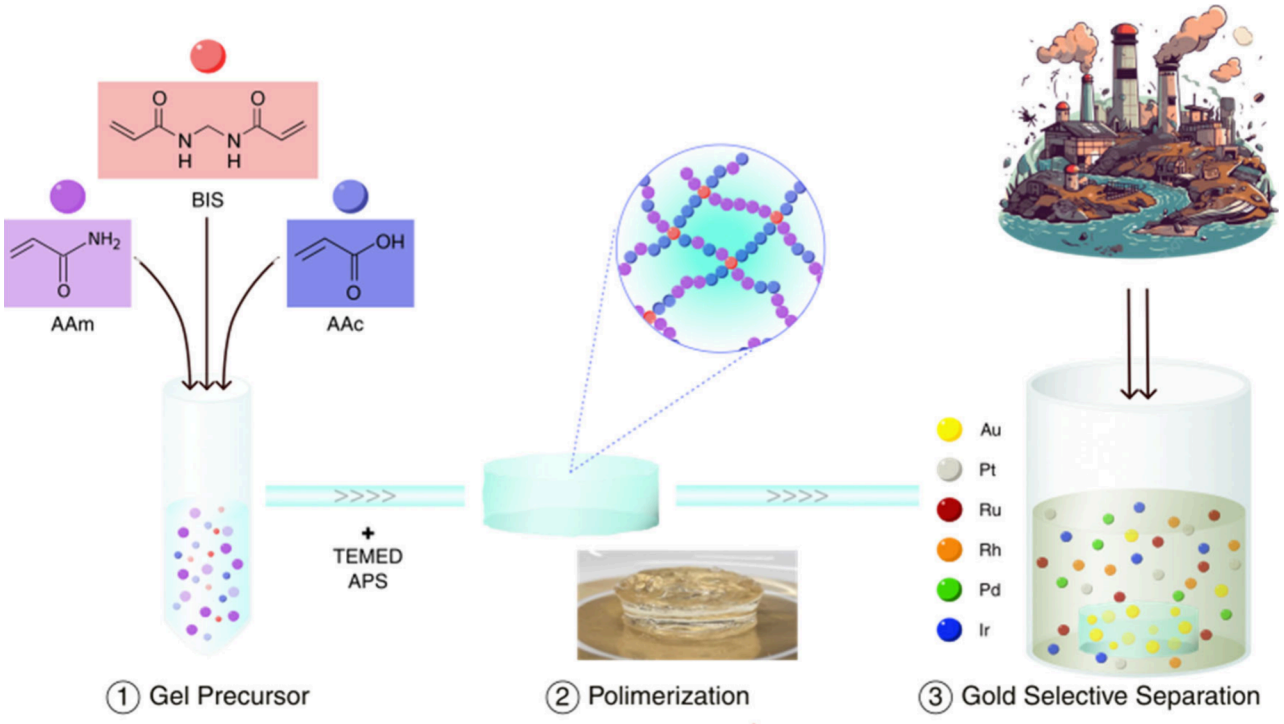

Figure 1. Scheme of the preparation of poly(AAm-co-AAc) hydrogels and their use for gold recovery. The selective gold adsorption could be conducted in different industrial wastewaters containing competing cations.

especially in large scale processes, resulting in potential water pollution and increased costs for wastewater remediations.

In between different organic adsorbents,[11−13] hydrogel-based ones have been considered as potential alternatives; these materials are formed by three-dimensional polymeric networks that can absorb significant amounts of water while remaining insoluble due to chemical or physical cross-linking. Hydrogels can offer a good modulation of the absorption capacity and selectivity by manipulating the functional groups and the structure porosity thus enhancing available specific surface area.[14] For what concerns the gold recovery, both synthetic[15,16] and natural-based hydrogels have been reported.[17,18] In the last class, materials obtained from protein waste (e.g., amyloid nanofibrils,[4,19] persimmon peel[20] or hairs[21]) are the most studied toward circular economy, and selective recovery has been demonstrated with respect to many metals, including Cu, Ni, Pb, Zn, Cr, Fe, and Mn.[19] Less studied is the selectivity with other precious metals (such as Pt, Rh, Ir, Pd, and Ru) that, on the other hand, are still present in industrial wastewater. As an example, lysozyme-based membranes demonstrated an outstanding adsorption capacity for gold but no selectivity when the other platinum group precious metal ions are present in solution.[4]

In this study, we propose the use of hydrogel based on a cross-linked copolymer prepared by acrylamide and acrylic acid for the gold recovery. These materials are easy to make, thus allowing for easy scale up of their standardized preparation; the synthesis employs only low-cost commercial monomers and a classical free radical polymerization, thus allowing a scalable and reproducible procedure. Indeed the poly(acrylamide-co-acrylic acid) hydrogels have been already studied for water treatment, in particular, for the adsorption of different cationic dyes (e.g., Methylene blue, Methyl violet) and metals (including Fe^{3+}, Cr^{3+}, Hg^{2+}, Pb^{2+}, Cu^{2+}, Cd^{2+}) with main examples reported in Table 1. The pH plays a crucial role due to protonation/deprotonation of the functional groups and

https://doi.org/10.1021/acsami.4c15657
ACS Appl. Mater. Interfaces 2024, 16, 68368−68378

thus the adsorption performances. Metals are generally adsorbed with a pH above 5, while recovery in acid solution has been barely demonstrated. To the best of our knowledge, gold recovery had never been described with this kind of hydrogels. In the last part of the study, we demonstrate the gold recovery during a batch adsorption test on an industrial wastewater with different metal ions competing being present. The metal concentration was lower than 20 ppm and thus more difficult to treat with state-of-the-art methods. During the water treatment, the hydrogel allows a complete selectivity of gold recovery toward Pt^{4+}, Rh^{3+}, and Ir^{3+} and a good selectivity with respect to Pd^{2+} and Ru^{3+}. The overall characterization demonstrates the system as a promising adsorbent for the treatment of acid wastewater containing a complex mix of metal cations, such as those obtained by jewelry industries or by electronic waste dissolution.

2. RESULTS AND DISCUSSION

2.1. Material Design and Preparation. The choice for the hydrogel chemical structures has been based on recent studies that demonstrate how both acrylamide and acrylic acid can be used as a reducing agent for gold cation in solution to obtain gold nanoparticle.[29] Acrylamide can effectively stabilize gold colloids,[30] or it can be polymerized *in situ* to obtain composite hydrogels with homogeneously distributed nanoparticles.[31,32] In this case, the proposed mechanism involved a direct redox reaction between $HAuCl_4$ and the amide group, with the prior formation of protonated acrylamide and the $AuCl_4^-$ counterion, which facilitates electron transfer to the amine group.[31] Polyacrylic acid can act simultaneously as a reducing agent and gold nanoparticle stabilizer, resulting in a stable colloidal formulation.[33] Although in all these examples heating between 50 and 80 °C is typically required to accelerate gold reduction,[29−32] here we demonstrate that copolymers of acrylamide and acrylic acid can promote the nanoparticle formation also at room temperature.

The hydrogels, later referred to as poly(AAm-co-AAc), were prepared by free radical polymerization in an aqueous mixture containing acrylamide (AAm) as the main monomer, acrylic acid (AAc) as the comonomer, and N,N′-methylenebis-(acrylamide) (BIS) as the cross-linker.[34] The material preparation is depicted in Figure 1. Three different monomer formulations were prepared, and after the addition of ammonium persulfate (APS, as an initiator) and tetramethylethylenediamine (TEMED, as a co-initiator), the polymerization occurred.[35] In all cases, the monomer concentration was fixed at 2 M (in water), and the concentration of BIS was 20 mM. Within this paper, the hydrogels are noted as PAAx, where x is the molar concentration of acrylamide, and the different compositions are reported in Table 2. For instance, the material labeled PAA1.6 contains acrylamide with a concentration of 1.6 M andacrylic acid 0.4 M.

The ratio between the two comonomers was adjusted to investigate the potential impact of molecular composition on absorption capabilities and kinetics. Indeed, this parameter is also expected to modulate other physical and chemical properties, such as the swelling degree. The efficiency of the polymerization process has been controlled by gel fraction measurements reported in Table 2. The hydrogel containing the lower amount of acrylic acid (PAA1.6) presented an almost quantitative polymerization at room temperature, while for the others, heating at 60 °C was employed to obtain a high gel fraction (93%).

Table 2. Different Compositions of Poly(AAm-co-AAc) Hydrogels and Their Gel Fraction

	AAm (M)	AAc (M)	BIS (mM)	Gel fraction (%)
PAA1.6	1.6	0.4	20	99
PAA1	1	1	20	93
PAA0.8	0.8	1.2	20	93

Such materials can be used directly as adsorbents without the need for further chemical treatment. As depicted in Figure 1, various wastewater streams containing cationic metals could be treated by simple immersion of the hydrogel in an acid water bath. The treated wastewater should have originated from both industrial waste and the dissolution of metals from electronic waste, among other examples. As already explained in the Introduction, a special focus is to be placed on the selective recovery of one metal with respect to the other allowing for the possible recycling of pure species.

The metal recovery performances of a hydrogel (e.g., amount of metals, adsorption kinetic of and selectivity of specific metal with respect to the others) can be determined by the chemical groups available for the adsorption or metal reduction that in turn also influence its structure and swelling capability. In particular, the swelling behavior of poly(AAm-co-AAc) hydrogel is strongly influenced by environmental parameters, such as temperature and pH of the solution.[36,37] The water absorption capabilities of each poly(AAm-co-AAc) hydrogel are reported in Figure 2 both at neutral and acid pH.

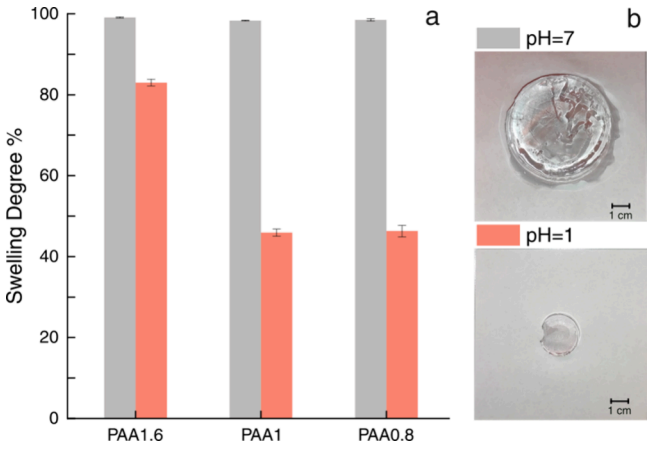

Figure 2. Swelling behavior of poly(AAm-co-AAc) hydrogels. (a) Swelling degree (equilibrium water content) of the hydrogels at different pH (gray bar: pH = 7; red bar: pH = 1). (b) Images of PAA1.6 treated in deionized water (pH = 7) and 0.2 M HCl solution (pH = 1), respectively.

The latter was selected since the industrial wastestream analyzed later presented a pH = 1. Solution at the same pH is also generally used when the metal cation solutions are obtained by e-waste dissolution;[19] thus, we believe to represent the more relevant case for gold recovery. The swelling degree was measured by gravimetric methods taking into account the maximum water content incorporated starting from the dry material at equilibrium, maintaining temperature and ionic strength of the buffer solution constant.

As expected, for all the materials, the swelling degree was greatly reduced by lowering the pH from 7 to 1. As an example, in PAA1.6, a reduction from 99% to 83% of the water

https://doi.org/10.1021/acsami.4c15657
ACS Appl. Mater. Interfaces 2024, 16, 68368−68378

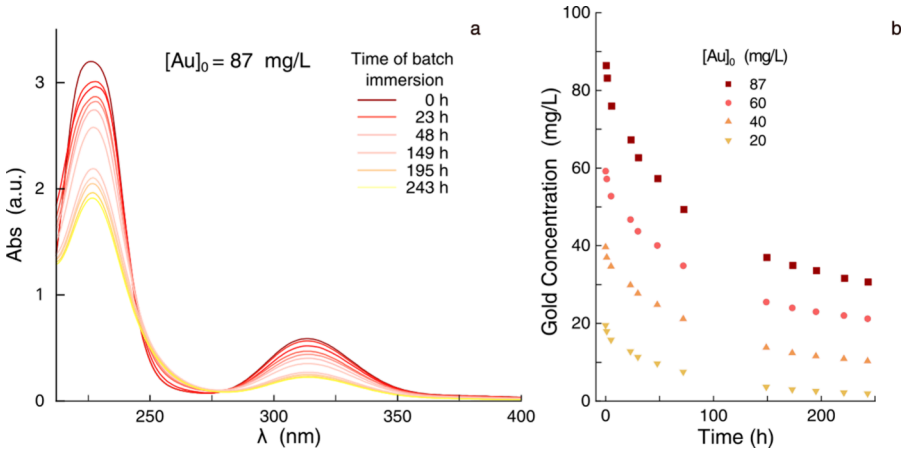

Figure 3. UV−vis absorption spectroscopy measures to monitor the gold absorption kinetics of the PAA1.6 hydrogel. (a) Example of absorbance measurements performed, each curve referring to an aliquot of treated pure gold solution at different times of PAA1.6 hydrogel immersion. (b) Residual gold concentration (mg/L) in solution as a function of time (h). Experimental conditions: pH 1, V_{sol} = 100 mL, m_{dry} = 300 mg.

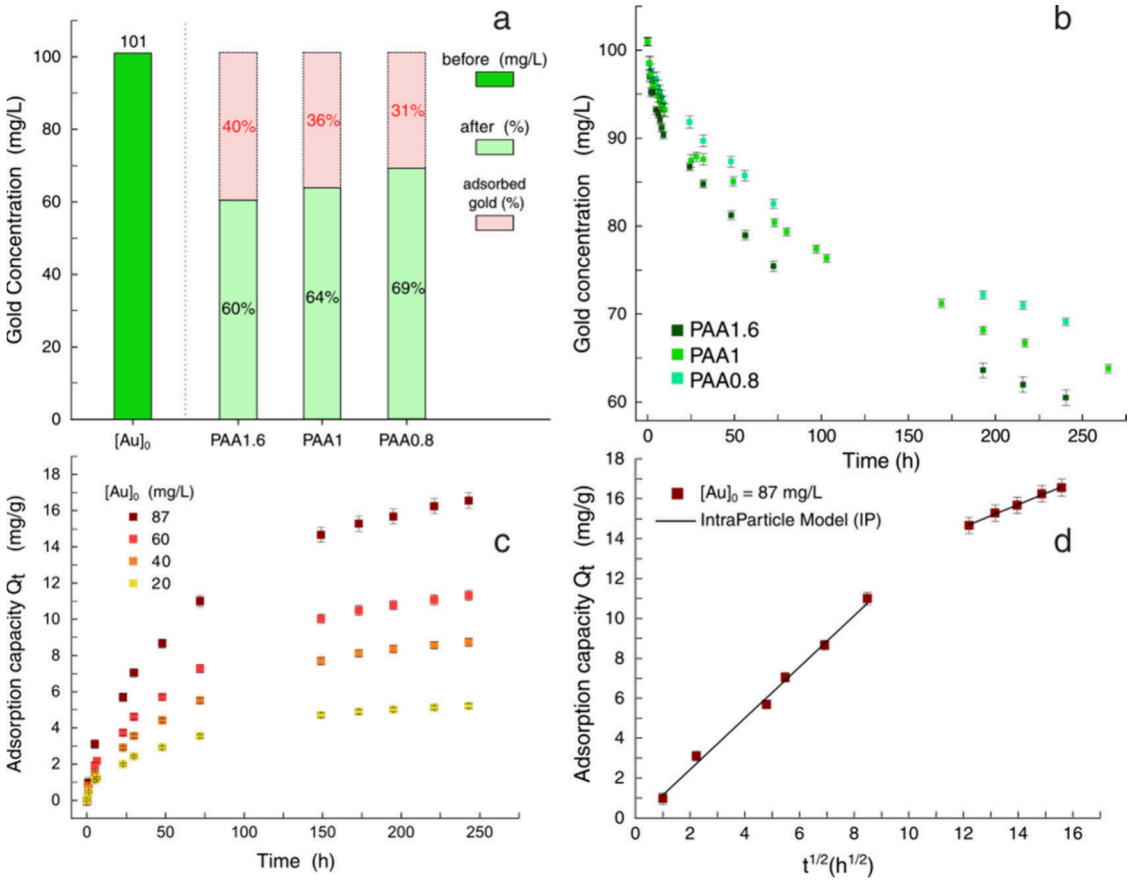

Figure 4. Comparison on gold removing performance. (a) Gold concentration in the solution before and after the hydrogel treatment. (b) Gold concentration decay in the gold solution treated with different hydrogels. (c) Adsorption capacity Q_t presented as a function of the PAA1.6 hydrogel immersion time at various starting concentrations of gold. (d) The adsorption kinetics model fitting (intraparticle model) relative to the highest starting concentration.

content was observed as an effect of carboxylic acid protonation. When pH ≤ pK_a, the carboxylic acid groups are not deprotonated (with the acrylic acid dissociation constant pK_a= 4.5),[38] and a lower swelling degree was observed. Increasing the amount of AAc content, a strong decrease in swelling degree at pH 1 was observed between PAA1.6 and PAA1 (83% and 45%, respectively) while further addition of AAc led only to small variation of water content. On the other hand, at pH = 7 (≥pK_a), the swelling capacity remains almost unchanged with increasing the acrylic acid content.[39]

2.2. Metal Ions Adsorption in Pure Gold Solutions. A detailed characterization of the gold adsorption capability and its kinetics was conducted using aqueous solutions obtained by dissolving $HAuCl_4$ salts (at pH = 1). The hydrogel was used for batch adsorption tests, where a specified amount of material was immersed in gold salt solutions at various

https://doi.org/10.1021/acsami.4c15657
ACS Appl. Mater. Interfaces 2024, 16, 68368−68378

Table 3. Fitted Kinetic Parameter Values of Different Stages for IP Model with the Associated Coefficient of Determination (R_i^2)[a,b]

C_0 (mg L^{-1})	$K_{I,1}$ (mg $g^{-1}h^{-1/2}$)	$S_{I,1}$ (mg g^{-1})	R_1^2	$K_{I,2}$ (mg g^{-1} $h^{-1/2}$)	$S_{I,2}$ (mg g^{-1})	R_2^2
20	0.514 ± 0.020	0.069 ± 0.05	0.994	0.182 ± 0.015	3.572 ± 0.203	0.981
40	0.741 ± 0.019	0.198 ± 0.0578	0.997	0.369 ± 0.032	4.968 ± 0.438	0.979
60	1.057 ± 0.040	−0.250 ± 0.118	0.994	0.459 ± 0.025	6.698 ± 0.342	0.991
87	1.603 ± 0.076	−0.279 ± 0.227	0.991	0.690 ± 0.024	9.574 ± 0.330	0.996

[a]Coefficients of the fitting processes are quantities computed as $R^2 = 1 - RSS/TSS$, with RSS being the "residual sum of squares" and TSS the "total sum of squares". The closer the data points are to the fitted curve, the smaller the *RSS* is. R^2 varies between 0 and 1; an R^2 value close to 1 indicates a good fitting model. [b]Experimental conditions: pH = 1, V_{sol} = 100 mL, PAA1.6 dry weight = 300 mg, room temperature (i.e., 25 °C).

concentrations (20, 40, 60, and 87 mg/L). The residual metal concentration in solution was monitored using UV−visible spectroscopy over an extended period, ranging from hours to days, as shown in Figure 3 for hydrogel PAA1.6. In particular, UV−vis absorbance measurements of the solution were monitored every hour (Figure 3a). The spectra display two distinct absorption bands in the UV spectral region. At pH < 4, Au(III) chloride exists in the planar $[AuCl_4]^-$ form,[40] giving rise to absorption bands at 229 and 315 nm as already reported.[41] In our study, the lower energy peak, corresponding to ligand−metal charge transfer, was chosen to monitor the changes in the concentration of the $AuCl_4^-$ ion during its adsorption on the hydrogel.

The absorbance variation was used to determine the final concentration according to the Lambert−Beer law, using $\varepsilon_{314\ nm}$ = (0.01209 ± 0.00008) cm^{-1} mg^{-1} L as the molar absorption coefficient of the gold salt (estimated by the calibration curve reported in Figure S1). In Figure 3b, the decay of the gold concentration as a function of time is reported for 250 h starting from the immersion of the PAA1.6 hydrogel. In all of the examples, we treated an initial volume of water (V_{sol}) of 100 mL with a mass of the dry hydrogel (m_{dry}) of 300 mg. As expected, the maximum amount of recovered gold and the adoption kinetics strongly depend on the initial salt concentration.

To study the influence of the chemical structures on the gold recovery, we studied the performances of three different hydrogels immersed in an aqueous solution of gold with a concentration of 101 mg/L for 250 h. Figure 4a compares the gold concentrations in the solution before and after the hydrogel treatments. Although there is a slight dependence on the adsorbent composition, the PAA1.6 sample results in a higher percentage of gold adsorption (40% with respect to the 36% and 31% recovered, respectively, by PAA1 and PAA0.8). Moreover, as shown in Figure 4b, PAA1.6 demonstrates quicker absorption kinetic. These results are also confirmed by additional absorption kinetic data reported in Figure S2 for solutions with a lower initial gold concentration (20 mg/L). In this case, the maximum percentage of adsorbed gold was about 66% from PAA1.6, while the other compositions adsorbed 52−53% of the initial metal content. These characterizations showed how the composition should play a role in the gold recovery with the better performance obtained by PAA1.6, particularly for low concentration solutions. Accordingly, this material was selected for further and more detailed adsorption kinetic studies reported in Figure 4c and d.

Figure 4c reports the trend as a function of time for the material adsorption capacity (Q_t), one of the most widely used parameters for characterizing and defining the adsorption performance for metals and dyes from aqueous solutions. Q_t was calculated by eq 1 as follows:

$$Q_t = (C_0 - C_t)\cdot V/m \quad (1)$$

where C_0 (mg/L) and C_t (mg/L) are the gold concentrations at time t_0 (before the hydrogel treatment) and t, respectively, V (L) is the volume of the solution, and m (g) is the weight of dry hydrogel.

As a straightforward consequence, the adsorption capacity at equilibrium (Q_e) is calculated considering the equilibrium gold concentration C_e as $C_{t=250h}$.

It is worth noting how the value of the adsorption capacity at equilibrium (Q_e) increases with the initial concentration of gold. Q_e values determined for PAA1.6 hydrogel by our analysis are 6.4, 10.6, 13.8, and 20.3 mg/g, respectively, for solutions with starting salt concentration of 20, 40, 60, and 87 mg/L. This trend, recently observed also for other systems,[42] is still opposite to the one of the collected gold percentage (with recovery percentage that increased at low concentration) making the poly(AAm-co-AAc) hydrogel particularly suitable for industrial waste solution treatment (with metals that should present in traces). Indeed, a higher Q_e has been found by increasing the initial salt concentration, with a value Q_e = 124 mg/g for a 800 mg/L gold solution as reported in Figure S3.

The adsorption kinetics occurring in these systems are typically complex, as they involve a series of dynamic steps that correspond to different mass transport phenomena during adsorption. According to a simplified yet effective framework, three primary dynamic steps can be identified in the process of adsorption in porous materials.[43] The first step involves the external diffusion of gold ions through the aqueous film surrounding the hydrogel driven by the concentration gradient between the bulk solution and the adsorbent surface. The second step involves the internal diffusion of ions within the hydrogel's pores, followed by the final step where ion adsorption occurs at the active sites of the adsorbent.

Among the various models, intraparticle diffusion models (IP) have been particularly effective in describing the adsorption kinetics of metal ions and other pollutants in porous materials. In the model, the kinetics is dominated by internal diffusion of ions, i.e., the second step previously introduced.

Among the IP models, the Weber and Morris model stands out as one of the most appropriate for characterizing adsorption kinetics in liquid environments. This model focuses exclusively on internal diffusion processes, addressing the dynamic problem by applying Fick's second law. According to this model, the time evolution of adsorption capacity, Q_t, can be described by eq 2:

$$Q_t = K_{intra}t^{1/2} + C \quad (2)$$

where K_{intra} is the kinetic constant of the process, and the C intercept is related to the mass transfer resistance across the

https://doi.org/10.1021/acsami.4c15657
ACS Appl. Mater. Interfaces 2024, 16, 68368−68378

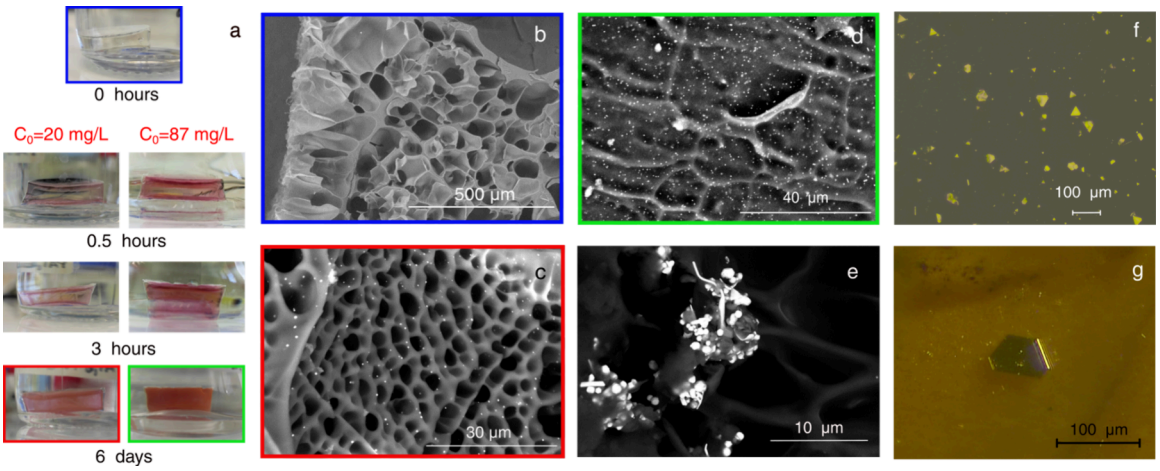

Figure 5. Formation of micrometric flakes and gold nanoparticles on the hydrogels. (a) Picture of PAA1.6 hydrogels during immersion in different gold concentrated solutions as a function of time. (b, e) SEM images of freeze-dried hydrogels before (b) and after immersion in a solution with initial gold concentration of 20 mg/L (c) or 87 mg/L (d, e). (f, g) Optical microscopy images of an hydrated hydrogel after gold adsorption.

liquid boundary layer. From our experimental data, we observed that the capacity kinetics show at least two different slopes in the linear plot of Q versus $t^{1/2}$, and these slopes can be the evidence of two consecutive stages of mass transport, where $S_{I,2}$ coincides with $Q_{t=t1}$. The adsorption kinetics of Figure 4d and Figure S4 have been described according to eqs 3:[44]

$$Q_t = K_{I,1}t^{1/2} + S_{I,1} \quad 0 \le t \le t_1$$
$$Q_t = K_{I,2}t^{1/2} + S_{I,2} \quad t_1 \le t \le t_2 \qquad (3)$$

When $t = t_1$, the first step of diffusion is completed, and adsorbates within the pores are assumed to be transferred to the active sites. Subsequently, other adsorbates from the solution can move into the pores. So migration of adsorbates from the liquid phase to the adsorbent internal surface occurs, and the hydrogel exhibits a new adsorption kinetic for $t > t_1$. This two-step process, according to our interpretation, describes two internal diffusion phases characterized by decreasing rates, as shown in Table 3, which contains the model parameters derived from fitting the experimental data to eqs 3. A similar behavior has been previously observed in other systems, where the double linear trend has been ascribed to the presence of multiple pore-size regimes.[45] The presence of multiple pore sizes is clearly evidenced by the SEM images in Figure 5. According to the Morris and Weber model, the intercept of the first stage, $S_{I,1}$, obtained by fitting the data, should have a negative value, and this is due to the mass transfer resistance (usually assumed as the resistance in the liquid boundary layer around the adsorbent to be tunnelled by the adsorbate).[45] On the other hand, as already reported,[44,46] where the constant $S_{I,1}$ value results are positive, the intercept is associated with the boundary layer effect, which can be considered as the first step of the entire kinetic adsorption process. The $S_{I,1}$ values reported in Table 3 are quite small but not zero for all tested initial gold concentrations; the positive intercepts leads us to consider the boundary layer effect as less relevant than the intraparticle diffusion process, which in turn leads to adsorption onto active sites present on the polymer network. This seems to suggest that some amount of the adsorbate is adsorbed by the hydrogel at the starting time of the measurement (the first gold concentration measurement in the solution is conducted 1 h after the hydrogel's immersion due to the limited sensitivity of UV−vis absorbance to detect small changes in adsorbed quantities over shorter time periods), suggesting that the positive intercept may simply reflect the limitations in the time resolution of the measurements. The values of $K_{I,1}$ and $K_{I,2}$ ranging from 0.2 to 1.6 (mg g^{-1} $h^{-1/2}$) are in the same scale of intraparticle diffusion constants evaluated for metal ions at similar concentrations.[46,47]

In addition to measuring the adsorption capacity, we also investigated a series of other experimental observables related to the processes occurring within the hydrogel. These observations enabled a more comprehensive understanding of the entire adsorption mechanism.

First, we observed that the gold ions are not only removed from the solution but also reduced to form elemental gold nanoparticles and microcrystalline flakes within the pores of the hydrogel. The presence of these nano- and microstructures of metallic gold is evidenced by the reddish coloration of the hydrogel, which is attributable to plasmonic surface resonance absorption (refer to Figure 5a).[31] This phenomenon can be further confirmed through direct observations using optical microscopy and scanning electron microscopy (SEM) imaging (see Figures 5b−g). In Figure 5a, we present images of the PAA1.6 hydrogel taken at different time intervals, illustrating the diffusion of gold nanoparticles throughout the adsorption process. The picture shows a progressive reddish color that appears inside the polymeric bulk material, for both the low (20 mg/L, left) and high (87 mg/L, right) gold concentration solutions. This colored region appeared first on the external part and then propagated throughout the whole hydrogel volume. Scanning electron microscope (SEM) analysis on the freeze-dried samples (without any other treatment), reported in Figure 5b−e, enables to observe the inner structures of the materials before the adsorption which present the typical microporous morphology of polyacrylamide hydrogels or similar[35] (Figure 5b). After the adsorption test, homogeneously distributed nanoparticles appeared on the surfaces of the polymeric networks. In the case of low gold concentration (C_0 = 20 mg/L), the hydrogel structure was nicely preserved also after the adsorption and gold reduction (Figure 5c), while for concentrations higher than C_0 = 60 mg/L the interaction

https://doi.org/10.1021/acsami.4c15657
ACS Appl. Mater. Interfaces 2024, 16, 68368−68378

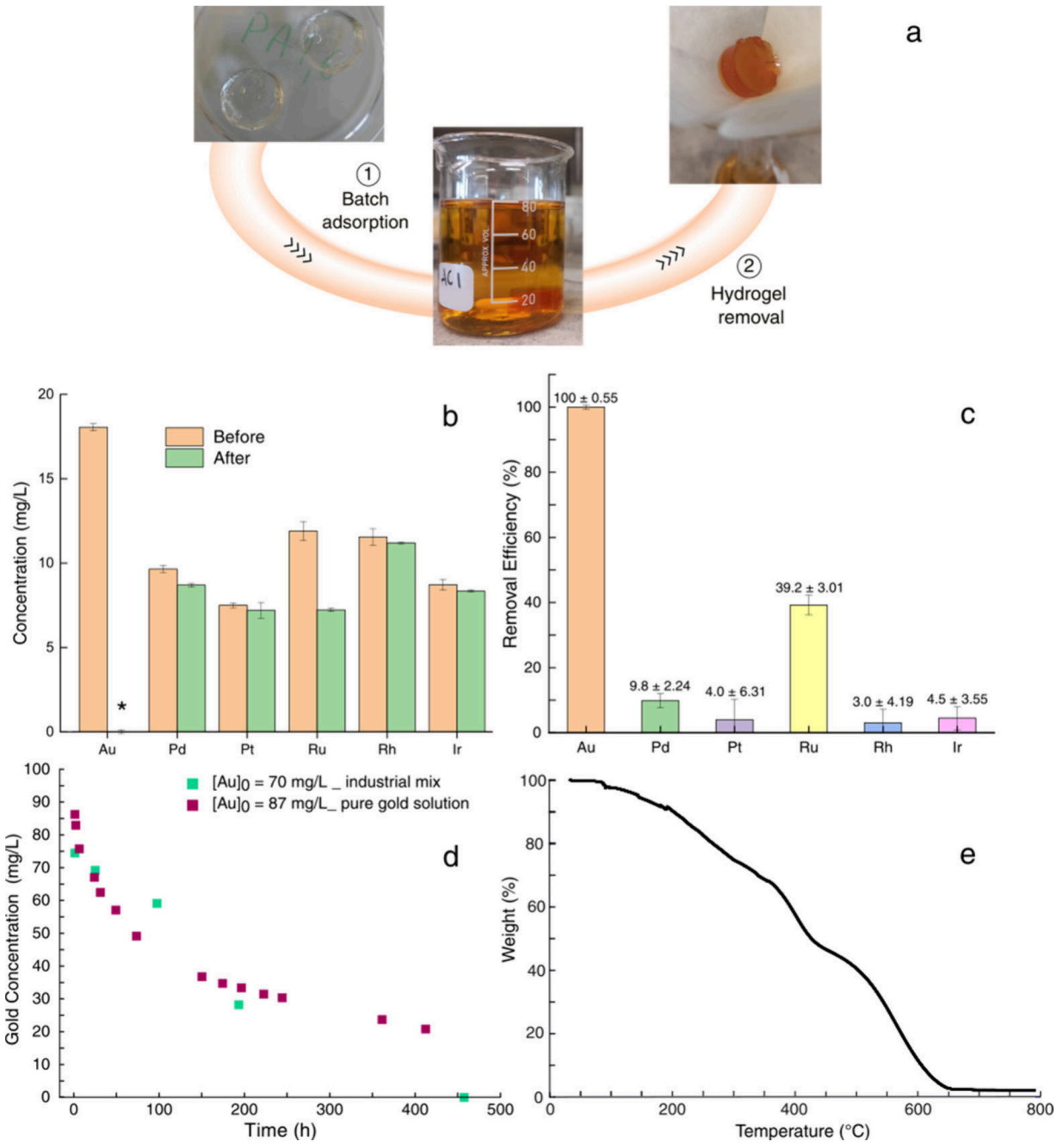

Figure 6. Treatment of mixed metal solutions with poly(AAm-co-AAC) hydrogels. (a) Steps for gold selective separation from a solution mimicking industrial waste. (b) Concentration of different metals in a mixed solution before and after PAA1.6 hydrogel treatment. Measures are performed by means of ICP-OES elemental analysis. (c) Percentage of metal ions recovery for PAA1.6 immersed (1 week) into the mixed metal solution. (d) Comparison of PAA1.6 hydrogel adsorption performances between a pure gold solution (red squares) measured by UV−vis spectroscopy and a mixed metal solution (turquoise squares) measured by ICP-OES. (e) Thermogravimetric analysis of PAA1.6 hydrogel matrix.

with gold was able to modify the 3D hydrogel structure resulting in a reduction of pore dimensions and partial closure of the pores (Figure 5d). This behavior suggests that gold is partially present in ionic form, coordinating with several functional groups located in the pore walls. Different samples are reported in Figures S5−S7; in all cases, we observed the same behavior. Regarding the nanoparticle size, in Figure 5e and Figure S8, we reported high magnification SEM that showed a high dispersion of the nanoparticle dimensions in the range from 50 nm up to hundreds of nm or more. Indeed, for samples treated in high gold concentration, formation of microplates was also observed, as shown in Figure 5f and g. The first is a polarized optical image where triangular and hexagonal structures can be detected with different sizes and showing birefringence, thus suggesting the formation of gold microcrystals.

Another important observation should be done in relation to the monomer composition. Indeed, the nanoparticle formation has been observed on all three matrices, to highlight how the application of poly(AAm-co-AAc) hydrogels avoided the use of any additional reducing agents for the recovery of gold in elemental form. Very interestingly, despite literature examples

https://doi.org/10.1021/acsami.4c15657
ACS Appl. Mater. Interfaces 2024, 16, 68368−68378

that need heating to form the nanoparticle on polyacrylamide or poly(acrylic acid) ,[30,31,33] our copolymerization approach allows the gold reduction spontaneously on the polymeric architecture at room temperature. The presence of acrylic acid seems to be critical for the process, as shown also in Figure S9, where a hydrogel composed only of the AAm monomer is compared with PAA1.6. After immersion in a gold solution, the formation of nanoparticles at room temperature was observed mainly in the second hydrogel (the one containing acrylic acid). On the other hand, the presence of acrylamide offers several benefits, including maintaining a high swelling degree at acidic pH (which improves diffusion and overall adsorption performance) and simplifying material preparation, as a high gel fraction can be achieved without the need for heating, which is otherwise required to polymerize acrylic acid.

2.3. An Example of Application: Gold Adsorption in a Mixed Metal Industrial Wastewater. The final step of this work is the use of the selected poly(AAm-co-AAc) hydrogel matrix (PAA1.6) as adsorbent in a mixed noble metal ion solution which closely mimics the realistic condition of an industrial wastewater, chosen on the basis of Cabro S.p.A. water residue. The target solution includes different precious metal ions (Au^{3+}, Pd^{2+}, Pt^{4+}, Ru^{3+}, Rh^{3+}, and Ir^{3+}) at quantities not exceeding 20 mg/L for each metal and determines the working conditions in an acid environment (pH = 1). The major challenges for the treatment of this type of solution is the selective recovery of one metal with respect to the others, together with a low metal concentration that reduces the number of available treatment techniques. Indeed, recent works on hydrogel absorbent demonstrated a high quantity of recovered gold but without selectivity when the metals of platinum group are present.[4]

In this regard, our hydrogel may offer an advantage if the primary mechanism for gold recovery is nanoparticle reduction rather than complexation or electrostatic interactions between the ions and the functional groups of the adsorbent. Under these conditions, selectivity is achieved if the proposed material reduces gold ions without affecting other metal cations. The already demonstrated gold adsorption has been obtained at a pH around 1 allowing, at least in principle, to eliminate the adsorption of the other metal ions due to high matrix effect interaction (e.g., acrylic acid is protonated disfavoring interaction with cations).[48] The treatment of the mixed metal solution followed a batch test, where the hydrogel is directly immersed in the solution for different times (Figure 6a). After 1 week, the initial orange solution became almost colorless, while the hydrogel changed color (see Figure S10). A detailed quantification of the metal concentration after hydrogel adsorption is reported in Figure 6b, while the relative recovery percentages are shown in Figure 6c. In this case, the concentration of each metal has been determined by ICP-OES (inductively coupled plasma-optical emission spectrometry) elemental analysis since the application of UV−visible spectroscopy was not possible for this complex solution.

After 1 week immersion, PAA1.6 was able to adsorb almost completely the gold present in the solution (recovery of 18 mg/L) with the formation of micro- and nanoparticles (see Figure S11 for SEM images). As supposed initially, the recovery occurs with high selectivity with respect to the competing cations. Indeed, cations like Pt^{4+}, Rh^{3+}, and Ir^{3+} were not adsorbed on PAA1.6, while Pd^{2+}, Ru^{3+} were adsorbed only in low amounts (0.8 and 5.7 mg/L, respectively, which correspond to 9.8% and 39% of recovery). After 4 days of treatment, the extraction selectivity of Au^{3+} over other adsorbed metals can be calculated as 55.07 times more selective over Pd^{2+} and 35.56 times over Ru^{3+}.

The same analysis conducted at different immersion times is reported in Figure S12. Indeed, after 24 h, the gold recovery was about 36.5%, and after 72 h, the percentage was increased at 98.3%. During this time, also the ruthenium was gradually adsorbed (recovery 22% and 40.9% at 24 and 72 h) demonstrating how the adsorption processes of the two metals are simultaneous. Thus, diminishing the immersion time of the hydrogel did not significantly improve the selectivity. Regarding the adsorption kinetics, Figure 6d shows the comparison between the hydrogel adsorption performance in a pure gold solution and in a mixed solution (containing gold with a similar concentration). The adsorption trends are quite similar, despite these measurements being performed using different techniques, UV−vis spectroscopy and ICP-OES. A difference was observed in the residual gold concentration; in the mixed solution, the hydrogel achieved complete recovery (within the detection limits of the ICP-OES analysis used), suggesting the potential for recovery even at lower concentrations. A final consideration regarding the potential use of poly(AAm-co-AAc) hydrogel pertains to the ultimate gold recovery from the material. This process could be carried out either by dissolving the formed nanoparticles or by thermally degrading the matrices to recover the solid metals. Regarding the former, an example of gold elution by aqua regia immersion is shown in Figure S13, but this approach results in an acidic solution with high metal dilution. For the latter, it is important to choose the matrix appropriately since it must lead to a low amount of solid carbon residue (ideally zero residue) after combustion. An insight into this aspect is shown by the thermogravimetric analysis (TGA) reported for PAA1.6 in Figure 6e. The hydrogel has already lost 50% of its original (dry) weight at 400 °C, and no solid residue is observed at 600 °C. A comparison with a commercial resin used for metal recovery is presented in Figure S14. The TGA analysis revealed a potential issue with the combustion of commercial materials (i.e., MTC1500 industrial resin), which is related to their formulation. On one hand, composite formulations can enhance adsorption capacity (albeit without metal selectivity); on the other hand, the high solid residue remaining after thermal treatment poses a significant challenge, hindering the recovery of solid metals with high purity.

Toward potential industrial scalability, a preliminary cost evaluation highlights the promising economic viability of our system. The total cost of producing the hydrogel required to recover 1 g of gold is below 0.1 € (based on the maximum Q_e reported in this study, see Table S1). Notably, the whole recovery process is energy efficient as no heating or cooling is necessary for both the polymerization of PAA1.6 and the adsorption process. Additionally, the wastewater can be conducted without the need for further chemical treatment (e.g., pH adjustment). This aspect represents a clear advantage when comparing our adsorbents with the conventional methods, such as activated carbon and ion exchange resins. Our hydrogels offer an effective and low-cost approach for the removal of heavy and precious metals, and with further optimization—such as by modulating the functional groups to expand the range of adsorbed species—our system has the potential for long-term use through recycling after gold elution, making it a highly competitive alternative for industrial applications.

https://doi.org/10.1021/acsami.4c15657
ACS Appl. Mater. Interfaces 2024, 16, 68368−68378

3. CONCLUSIONS

In summary, we demonstrated how hydrogels prepared by the copolymerization of acrylamide and acrylic acid can be used as efficient adsorbents for gold ions in acid solutions. The materials demonstrated the ability to reduce this metal, forming particles of various sizes, ranging from 50 nm nanoparticles to microplates several hundred micrometers in size, all of which were homogeneously dispersed within the polymeric matrices. This process was effective even at concentrations lower than 20 mg/L. The hydrogel's inherent reduction capability eliminated the need for additional reductants, offering a significant advantage in reducing the environmental impact associated with the use of reducing agents and energy consumption. Moreover, the behavior observed here for metal recovery could also be used for the synthesis of nanoparticle catalysts that are well-dispersed and supported within a polymeric matrix.

A remarkable feature of poly(AAm-co-AAC) is the possibility to obtain a good separation of gold by other precious metals present in the solution, a behavior which is rarely reported on other hydrogels used for gold recovery. We hypothesize that selectivity is mainly driven by the recovery mechanism of the hydrogel, where the gold reduction occurs at acid pH while other metals remain unaffected. At this pH, interactions such as electrostatic binding and complexation between the functional groups and other ions are less favored. Our systems allowed for a complete selectivity from cations like Pt^{4+}, Rh^{3+}, or Ir^{3+} and a good selectivity toward Pd^{2+} and Ru^{3+}. The higher limitation for specific adsorption is represented by the presence of ruthenium with a ratio of 0.31 in weight of the adsorbed metals (in the proposed example). Indeed, further studies should be conducted to efficiently remove one of the two metals by the hydrogel matrices by appropriate elution to achieve complete metal separation. The dissolution of metals, including elemental gold, is a key aspect for enabling reuse of the hydrogel in multiple adsorption cycles. Although this study demonstrates gold dissolution using aqua regia, simpler and more environmentally friendly methods are necessary to enable effective adsorbent recycling. Future efforts will focus on introducing additional chemical groups to modify selectivity, potentially enabling the recovery of other precious metals, for example, under different pH conditions. As a final remark, we would like to emphasize that the present hydrogels are already suitable for gold recovery in various applications, including metal recycling from e-waste and treatment of residues from the jewelry industries.

4. EXPERIMENTAL SECTION

4.1. Materials. Acrylamide (AAm), acrylic acid (AAc), N,N′-methylenebisacrylamide (BIS), ammonium persulfate (APS), tetramethylethylenediamine (TEMED), tetrachloroauric(III) acid trihydrate ≥99.9% ($HAuCl_4{\cdot}3H_2O$), and hydrochloric acid (HCl) were purchased from Sigma-Aldrich. All chemicals appearing in this work were utilized without any further manipulation. All other metal salts (containing Pt^{4+}, Rh^{3+}, Ir^{3+}, Pd^{2+}, and Ru^{3+}) have been provided by Cabro S.p.A.

4.2. Hydrogel Synthesis. A solution of monomers (AA and AC in different ratios reported in Table 2) and BIS was prepared with deionized water. Then, a 10% m/V solution of APS was added to achieve a final concentration of 0.2% of initiator, and a 10% m/V solution of TEMED was added to achieve a final concentration of 2% The free-radical polymerization occurred in 1 h at room temperature for PAA1.6 and at 60 °C PAA1 and PAA0.8.

4.3. Hydrogel Characterization. The gel fraction (GF) indicates the percentage of solid monomers that effectively are incorporated inside the network. It was calculated using the following equation:

$$GF(\%) = (Wd_2/Wd_1)\times 100 \quad (4)$$

where Wd_1 (g) and Wd_2 (g) are the weight of the dry material just after its preparation (Wd_1) and the weight of the dried gel after immersion in water (to eliminate unpolymerized material, Wd_2).

The swelling degree (SD) indicates the percentage of water retained by the gel network in its fully swollen state. It was calculated by the following equation:

$$SD(\%) = (Ws - Wd)/Ws \times 100 \quad (5)$$

where Ws(g) and Wd(g) are, respectively, the weight of the fully swollen hydrogel and the weight of completely dried hydrogel, respectively. The measurements were repeated in triplicate and under two different pH conditions (neutral and strongly acid buffer solution). Polarized optical microscopy (AxioLab5, Zeiss) (POM) and scanning electron microscopy (FlexSEM 1000, Hitachi) (SEM) images were performed to characterize the internal structure of the hydrogel before and after metal ions adsorption. The thermogravimetric measurements have been performed using a SDT Q600, T.A. Instruments thermogravimetric analyzer, furnished by Cabro S.p.A industry. The measures were carried out in a temperature range from 20 to 800 °C, with a heating rate of 2 °C/min under an air atmosphere.

4.4. Metal Ions Adsorption Measurements. The batch adsorption tests were performed by immersion of the hydrogel (after swelling of 300 mg of dry materials) in 100 mL of solution with different initial gold concentrations (20, 40, 60, 87 mg/L) or mixed metal ions solution. The gold solutions were prepared by dissolving tetrachloroauric(III) acid ($HAuCl_4$) in a previously prepared 0.2 M HCl buffer. The final pH of the solution was adjusted to pH = 1. The measures of residual gold concentration in pure gold solutions were performed by means of UV−vis spectroscopy (LAMBDA 950 UV/vis spectrophotometer, PerkinElmer; V650 UV/vis spectrophotometer, JASCO - Grenoble). The mixed metal cation solution has been furnished by Cabro S.p.A., starting from disposal of precious metal ion solutions already existing in the company. In this case, the technique used to follow the residual metal concentration is ICP-OES spectroscopy elemental analysis (5110 ICP-OES, Agilent, measures provided by Cabro S.p.A.). Selectivity of Au^{3+} extraction over other adsorbed metals in the mixed solution is calculated according to the following equation:

$$\text{Selectivity of } Au^{3+} \text{over other metal } M^{+} = (C(M)_{final}/C(Au)_{final})/(C(M)_{initial}/C(Au)_{initial}) \quad (6)$$

where $C(M)_{final}$ and $C(M)_{initial}$ are, respectively, the concentrations of the metal M before and after the adsorption process.

■ ASSOCIATED CONTENT

Supporting Information

The Supporting Information is available free of charge at https://pubs.acs.org/doi/10.1021/acsami.4c15657.

Gold molar extinction coefficient estimation; further details on gold recovery kinetics and model fitting; further SEM images of PAA1.6 matrix before and after the metal adsorption; comparison of TGA of PAA1.6 and MTC1500 industrial resin; production cost estimation (PDF)

■ AUTHOR INFORMATION

Corresponding Authors

Alice Boschetti − *European Laboratory for Non-Linear Spectroscopy (LENS), 50019 Sesto Fiorentino, Italy; Istituto Nazionale di Ricerca Metrologica (INRiM), 10135 Torino,*

https://doi.org/10.1021/acsami.4c15657
ACS Appl. Mater. Interfaces 2024, 16, 68368−68378

Italy; orcid.org/0000-0001-5531-6924; Email: a.boschetti@inrim.it
Daniele Martella − *European Laboratory for Non-Linear Spectroscopy (LENS), 50019 Sesto Fiorentino, Italy; Dipartimento di Chimica "Ugo Schiff", Università di Firenze, 50019 Sesto Fiorentino, Italy*; orcid.org/0000-0002-8845-0908; Email: daniele.martella@unifi.it

Authors

Pamela Cinfrignini − *European Laboratory for Non-Linear Spectroscopy (LENS), 50019 Sesto Fiorentino, Italy; Dipartimento di Fisica e Astronomia, Università di Firenze, 50019 Sesto Fiorentino, Italy*
Giacomo Ghini − *Cabro S.p.A, 52100 Arezzo, Italy*
Alice Tenti − *Cabro S.p.A, 52100 Arezzo, Italy*
Marie Plazanet − *Laboratoire Interdisciplinaire de Physique, Université Joseph Fourier, 38000 Grenoble, France*; orcid.org/0000-0002-7041-8299
Renato Torre − *European Laboratory for Non-Linear Spectroscopy (LENS), 50019 Sesto Fiorentino, Italy; Dipartimento di Fisica e Astronomia, Università di Firenze, 50019 Sesto Fiorentino, Italy*; orcid.org/0000-0003-3182-9906

Complete contact information is available at: https://pubs.acs.org/10.1021/acsami.4c15657

Author Contributions

P.C., A.B., D.M., M.P., and R.T. conceived the experiments. P.C. conducted the experiments and analyzed the results. A.B., D.M., M.P., A.T., and G.G. provided support and supervision for the experiments and analysis. P.C. wrote the main manuscript and prepared the figures, with contributions from D.M. and A.B. All authors reviewed the manuscript.

Notes

The authors declare no competing financial interest.

■ ACKNOWLEDGMENTS

This research was funded by Next Generation EU Programme: project PRIN-2022JWAF7Y and I-PHOQS Infrastructure [IR0000016, ID D2B8D520, CUP B53C22001750006], European Union's Horizon 2020 research and innovation program under grant agreement no. 871124 Laserlab-Europe and by the project CNR-FOE-LENS-2023. P.C. acknowledges the European Union - PON Research and Innovation 2014-2020 (DM 1061/2021) for funding her Ph.D. research contract.

■ REFERENCES

(1) Ullah, F.; Othman, M. B. H.; Javed, F.; Ahmad, Z.; Akil, H. M. Classification, processing and application of hydrogels: A review. *Materials Science and Engineering: C* **2015**, *57*, 414−433.
(2) Gold Demand Trends Full Year 2023. *World Gold Council*. https://www.gold.org/goldhub/research/gold-demand-trends/gold-demand-trends-full-year-2023#:~:text=Another%20year%20of%20blistering%20central,on%20record%20at%204%2C899t (accessed 2024−09−01).
(3) Distribution of gold demand worldwide in 2023, by sector. *Statista*. https://www.statista.com/statistics/299609/gold-demand-by-industry-sector-share/ (accessed 2024−09−01).
(4) Yang, F.; Yan, Z.; Zhao, J.; Miao, S.; Wang, D.; Yang, P. Rapid capture of trace precious metals by amyloid-like protein membrane with high adsorption capacity and selectivity. *J. Mater. Chem. A* **2020**, *8*, 3438−3449.
(5) Syed, S. Recovery of gold from secondary sources—A review. *Hydrometallurgy* **2012**, *115*−*116*, 30−51.
(6) Barman, M. K.; Bhattarai, A.; Saha, B. Applications of ion exchange resins in environmental remediation. *VJCH* **2023**, *61*, 533−550.
(7) Rengaraj, S.; Yeon, K. H.; Moon, S. H. Removal of chromium from water and wastewater by ion exchange resins. *Journal of Hazardous Materials* **2001**, *87* (1), 273−287.
(8) Van Deventer, J. New Developments in Ion Exchange Resins for the Recovery of Gold in Complex Ores. *Hydrometallurgy* **2014**, *1*, 677.
(9) Bolisetty, S.; Peydayesh, M.; Mezzenga, R. Sustainable technologies for water purification from heavy metals: review and analysis. *Chem. Soc. Rev.* **2019**, *48*, 463−487.
(10) Ahamed, M. E. H.; Mulaba Bafubiandi, A. F.; Marjanovic, L.; Mbianda, X. Y. Recovery of gold from mining solutions using Au (III)-imprinted polymeric resins with pyridine, ethylenediamine and aminothiophosphate functionalities. *Mineral Processing and Extractive Metallurgy*. **2019**, *128* (4), 221−238.
(11) Dai, Y.; Zheng, K.; Tan, Y.; Xiang, W.; Xianyu, B.; Xu, H. Fischesserite-Inspired Recyclable Se-Polyurethanes for Selective Gold Extraction. *Adv. Sustainable Syst.* **2020**, *4*, No. 2000072.
(12) Liu, W.; Jones, L. O.; Wu, H.; Stern, C. L.; Sponenburg, R. A.; Schatz, G. C.; Stoddart, J. F. Supramolecular Gold Stripping from Activated Carbon Using α-Cyclodextrin. *J. Am. Chem. Soc.* **2021**, *143*, 1984.
(13) Wu, H.; Wang, Y.; Tang, C.; Jones, L. O.; Song, B.; Chen, X.-Y.; Zhang, L.; Wu, Y.; Stern, C. L.; Schatz, G. C.; Liu, W.; Stoddart, J. F. High-efficiency gold recovery by additive-induced supramolecular polymerization of β-cyclodextrin. *Nat. Commun.* **2023**, *14*, 1284.
(14) Xiang, Y.; Liu, Y.; Li, M.; Bai, W.; Liu, G.; Xu, L. The recovery of Au(III) by hydrogel-like beads. *Hydrometallurgy* **2023**, *215*, No. 105964.
(15) Kılıc, A. G.; Malcı, S.; Celikbıcak, O.; Sahiner, N.; Salih, B. Gold recovery onto poly(acrylamide-allylthiourea) hydrogels synthesized by treating with gamma radiation. *Anal. Chim. Acta* **2005**, *547* (1), 18−25.
(16) Khozemy, E. E.; Nasef, S. M.; Mohamed, T. M. Radiation Synthesis of Superabsorbent Hydrogel (Wheat Flour/Acrylamide) for Removal of Mercury and Lead Ions from Waste Solutions. *J. Inorg. Organomet Polym.* **2020**, *30*, 1669−1685.
(17) Peydayesh, M.; Mezzenga, R. Protein nanofibrils for next generation sustainable water purification. *Nat. Commun.* **2021**, *12*, 3248.
(18) Bolisetty, S.; Mezzenga, R. Amyloid−carbon hybrid membranes for universal water purification. *Nat. Nanotechnol.* **2016**, *11*, 365−371.
(19) Peydayesh, M.; Boschi, E.; Donat, F.; Mezzenga, R. Gold Recovery from E-Waste by Food-Waste Amyloid Aerogels. *Adv. Mater.* **2024**, *36*, No. 2310642.
(20) Parajuli, D.; Kawakita, H.; Inoue, K.; Ohto, K.; Kajiyama, K. Persimmon peel gel for the selective recovery of gold. *Hydrometallurgy* **2007**, *87*, 133−139.
(21) Yu, D.; Morisada, S.; Kawakita, H.; Sakaguchi, K.; Osada, S.; Ohto, K.; Inoue, K.; Song, X. M.; Zhang, G.; Sathuluri, R. R. Gold recovery from precious metals in acidic media by using human hair waste as a new pretreatment-free green material. *Journal of Environmental Chemical Engineering* **2021**, *9*, No. 104724.
(22) Lv, Q.; Shen, Y.; Qiu, Y.; Wu, M.; Wang, L. Poly(acrylic acid)/poly(acrylamide) hydrogel adsorbent for removing methylene blue. *J. Appl. Polym. Sci.* **2020**, *137*, No. 49322.
(23) Wang, Y.; Zeng, L.; Ren, X.; Song, H.; Wang, A. Removal of Methyl Violet from aqueous solutions using poly (acrylic acid-*co*-acrylamide)/attapulgite composite. *Journal of Environmental Sciences* **2010**, *22*, 7−14.
(24) Li, D.; Zhan, W.; Zuo, W.; Li, L.; Zhang, J.; Cai, G.; Tian, Y. Elastic, tough and switchable swelling hydrogels with high entanglements and low crosslinks for water remediation. *Chemical Engineering Journal* **2022**, *450*, No. 138417.
(25) Orozco-Guareño, E.; Santiago-Gutiérrez, F.; Morán-Quiroz, J. L.; Hernandez-Olmos, S. L.; Soto, V.; de la Cruz, W.; Manríquez, R.; Gomez-Salazar, S. Removal of Cu (II) ions from aqueous streams

using poly(acrylic acid-co-acrylamide) hydrogels. *J. Colloid Interface Sci.* **2010**, *349*, 583−593.
(26) Chowdhury, N.; Solaiman; Roy, C. K.; Firoz, S. H.; Foyez, T.; Imran, A. B. Role of Ionic Moieties in Hydrogel Networks to Remove Heavy Metal Ions from Water. *ACS Omega* **2021**, *6* (1), 836−844.
(27) Zendehdel, M.; Barati, A.; Alikhani, H. Removal of heavy metals from aqueous solution by poly(acrylamide-co-acrylic acid) modified with porous materials. *Polym. Bull.* **2011**, *67*, 343−360.
(28) Zhao, B.; Jiang, H.; Lin, Z.; Xu, S.; Xie, J.; Zhang, A. Preparation of acrylamide/acrylic acid cellulose hydrogels for the adsorption of heavy metal ions. *Carbohydr. Polym.* **2019**, *224*, No. 115022.
(29) Bai, J.; Li, Y.; Du, J.; Wang, S.; Zheng, J.; Yang, Q.; Chen, X. One-pot synthesis of polyacrylamide-gold nanocomposite. *Mater. Chem. Phys.* **2007**, *106*, 412−415.
(30) Tatarchuk, V. V.; Dobrolyubova, Y. O.; Druzhinina, I. A.; Zaikovskii, V. I.; Gevko, P. N.; Maksimovskii, E. A.; Gromilov, S. A. Facile synthesis of gold nanoparticles in aqueous acrylamide solution. *Russ. J. Inorg. Chem.* **2016**, *61*, 535−543.
(31) Tatarchuk, V.; Gromilov, S.; Plyusnin, P. One-step synthesis and characterization of gold nanoparticles doped polyacrylamide hydrogels. *J. Sol-Gel Sci. Technol.* **2024**, *110*, 377−390.
(32) Song, Y.; Li, Z.; Wang, L.; Yao, Y.; Chen, C.; Cui, K. One-step preparation of hybrid materials of polyacrylamide networks and gold nanoparticles, Microsc. *Res. Technol.* **2008**, *71*, 409−412.
(33) Shabeeb, D.; Haider, A.; Mohammed, A. T. Synthesis of gold nanoparticles using Poly Acrylic Acid as reducing agent−Characterization and in vitro study of anticancer cervix (HELA) activity. *BEST: IJHAMS* **2017**, *4*, 2454−4728.
(34) Vassallo, M.; Vicentini, M.; Salzano De Luna, M.; Barrera, G.; Tiberto, P.; Manzin, A.; Martella, D. Magnetic Hyperthermia to Promote Acrylamide Radical Polymerizations. *ACS Applied Polymer Materials* **2024**, *6*, 4696−4707.
(35) Cappitti, A.; Palmieri, F.; Garella, R.; Tani, A.; Chellini, F.; Salzano De Luna, M.; Parmeggiani, C.; Squecco, R.; Martella, D.; Sassoli, C. Development of accessible platforms to promote myofibroblast differentiation by playing on hydrogel scaffold composition. *Biomaterials Advances* **2023**, *155*, No. 213674.
(36) Nesrinne, S.; Djamel, A. Synthesis, characterization and rheological behavior of pH sensitive poly(acrylamide-co-acrylic acid) hydrogels. *Arabian Journal of Chemistry* **2017**, *10*, 539−547.
(37) Thakur, A.; Wanchoo, R.; Singh, P. Structural Parameters and Swelling Behavior of pH Sensitive Poly(acrylamide-co-acrylic acid) Hydrogels. *Chem. Biochem. Eng. Q.* **2011**, *25* (2), 181−184.
(38) Li, W.; Zhao, H.; Teasdale, P. R.; John, R.; Zhang, S. Synthesis and characterisation of a polyacrylamide−polyacrylic acid copolymer hydrogel for environmental analysis of Cu and Cd. *React. Funct. Polym.* **2002**, *52*, 31−41.
(39) Chau, A. L.; Getty, P. T.; Rhode, A. R.; Bates, C. M.; Hawker, C. J.; Pitenis, A. A. Superlubricity of pH-responsive hydrogels in extreme environments. *Front. Chem.* **2022**, *10*, No. 891519.
(40) Peck, J. A.; Tait, C. D.; Swanson, B. I.; Brown, G. E. Speciation of aqueous gold (III) chlorides from ultraviolet/visible absorption and Raman/resonance Raman spectroscopies. *Geochim. Cosmochim. Acta* **1991**, *55* (3), 671−676.
(41) Wojnicki, M.; Rudnik, E.; Luty-Błocho, M.; Pacławski, K.; Fitzner, K. Kinetic studies of gold (III) chloride complex reduction and solid phase precipitation in acidic aqueous system using dimethylamine borane as reducing agent. *Hydrometallurgy* **2012**, *127−128*, 43−53.
(42) Naganeyama, Y.; Tsuruta, T. Removal, Recovery and Recycle of Gold (III) from Aqueous Solution Using Persimmon Tannin Gel. *International Journal of Geosciences* **2021**, *12* (12), 1084−1094.
(43) Wang, J.; Guo, X. Adsorption kinetic models: Physical meanings, applications, and solving methods. *Journal of Hazardous Materials* **2020**, *390*, No. 122156.
(44) Wang, J.; Guo, X. Rethinking of the intraparticle diffusion adsorption kinetics model: Interpretation, solving methods and applications. *Chemosphere* **2022**, *309*, No. 136732.
(45) Obradović, B. Guidelines for general adsorption kinetics modeling. *Hemijska industrija* **2020**, *74*, 65−70.
(46) Tang, S.; Lin, L.; Wang, X.; Feng, A.; Yu, A. Pb(II) uptake onto nylon microplastics: Interaction mechanism and adsorption performance. *Journal of Hazardous Materials* **2020**, *386*, No. 121960.
(47) Sera, P. R.; Diagboya, P. N.; Akpotu, S. O.; Mtunzi, F. M.; Chokwe, T. B. Potential of valourized Moringa oleifera seed waste modified with activated carbon for toxic metals decontamination in conventional water treatment. *Bioresource Technology Reports* **2021**, *16*, No. 100881.
(48) Taqui Khan, M. M.; Ramachandraiah, G.; Rao, A. P. Ruthenium (III) Chloride in Aqueous Solution: Electrochemical and Spectral Studies. *Inorg. Chem.* **1986**, *25*, 665−670.

https://doi.org/10.1021/acsami.4c15657
ACS Appl. Mater. Interfaces 2024, 16, 68368−68378